HHS Public Access

Author manuscript

Kidney Int. Author manuscript; available in PMC 2014 May 01.

Published in final edited form as:

Kidney Int. 2013 November ; 84(5): 950–961. doi:10.1038/ki.2013.197.

Podocyte-specific deletion of signal transducer and activator of transcription 3 attenuates nephrotoxic serum-induced glomerulonephritis

Yan Dai[1,2], **Leyi Gu**[3], **Weijie Yuan**[2], **Qing Yu**[2], **Zhaohui Ni**[3], **Michael J. Ross**[1], **Lewis Kaufman**[1], **Huabao Xiong**[4], **David Salant**[5], **John C. He**[1,6], and **Peter Y. Chuang**[1]

[1]Div. of Nephrology, Mount Sinai School of Medicine, New York, NY, US

[2]Div. of Nephrology, Shanghai First People's Hospital, Shanghai Jiaotong University School of Medicine, Shanghai, China

[3]Renal Division and Molecular Cell Laboratory for Kidney Disease, Renji Hospital, Shanghai Jiaotong University School of Medicine, Shanghai, China

[4]Immunobiology Center, Mount Sinai School of Medicine, New York, NY, US

[5]Renal Section, Boston University, Boston, MA, US

[6]Renal Section, James J. Peters Veterans Affairs Medical Center, Bronx, NY, US

Abstract

Activation of signal transducer and activator of transcription (STAT)3 correlates with proliferation of extra-capillary glomerular epithelial cells and the extent of renal injury in glomerulonephritis. To delineate the role of STAT3 in glomerular epithelial cell proliferation we examined the development of nephrotoxic serum-induced glomerulonephritis in mice with and without podocyte-restricted STAT3 deletion. Mice with STAT3 deletion in podocytes developed less crescents and loss of renal function compared to those without STAT3 deletion. Proliferation of glomerular cells, loss of podocyte markers, and recruitment of parietal epithelial cells were found in nephritic mice without STAT3 deletion, but mitigated in nephritic mice with podocyte STAT3 deletion. Glomerular expression of pro-inflammatory STAT3 target genes was significantly reduced in nephritic mice with, compared to those without, podocyte STAT3 deletion. However, the extent of glomerular immune complex deposition was not different. Podocytes with STAT3 deletion were resistant to interleukin-6-induced STAT3 phosphorylation and pro-inflammatory STAT3 target gene expression. Thus, podocyte STAT3 activation is critical for the development of crescentic glomerulonephritis.

Correspondence: Peter Y. Chuang, Mount Sinai School of Medicine, Department of Medicine, Division of Nephrology, One Gustave L Levy Place, Box 1243, New York, NY 10029, USA. Tel: 212-659-1752; Fax: 212-831-0114. peter.chuang@mssm.edu.

Disclosure:

The authors have no competing financial interests to disclose.

Keywords

Glomerulonephritis; podocyte; signaling; glomerulus; proliferation

Introduction

Accumulation of hyperplastic glomerular epithelial cells in Bowman's space is observed in both crescentic glomerulonephritis (GN) and collapsing glomerulopathy. Crescentic glomerulonephritis occurs in a wide range of kidney diseases, including IgA nephropathy, anti-glomerular basement membrane GN, anti-neutrophil cytoplasmic antibody-mediated GN, lupus nephritis, and type I membranoproliferative GN[1]. Collapsing glomerulopathy is observed in patients with HIV-1 seropositivity[2], other viral infections[3, 4], pamidronate toxicity[5], and de novo or recurrent idiopathic collapsing glomerulopathy in the renal allograft[6]. Although histologic features of these two entities are different—crescentic GN[7] is characterized by inflammatory changes in glomerular capillaries with focal or diffuse necrosis of glomerular capillaries, while collapsing glomerulopathy[8] is associated with segmental to global collapse of the glomerular capillary tuft—extracapillary proliferation of glomerular epithelial cells is observed in both conditions.

Presence of glomerular crescents on kidney biopsy is associated worse prognosis in patients with glomerulonephritis[9]. Recent studies of human and animal model of crescentic GN have documented the accumulation of podocytes[10–12] as well as parietal epithelial cells (PECs)[13, 14] in crescentic lesions. In addition to collapsing glomerulopathy and crescentic GN, prominent epithelial cell proliferation has also been observed in murine models where the primary cell-specific stimulus/insult was directed to either the podocyte[11, 15] or PEC[16]. These findings provide additional evidence that injury to either glomerular epithelial cell type could precipitate glomerular epithelial cells (podocytes, PECs or both) to proliferate and form cellular crescents. Signaling pathways orchestrating this proliferative response in crescent formation, however, have been not characterized.

Signal transducers and activators of transcription (STAT)-mediated signaling is involved in the regulation of cell proliferation and inflammation[17]. STAT3 signaling is activated in kidneys of mice[18] and human[19] with GN. Furthermore, activation of podocytes STAT3 has also been shown to drive the proliferation and dedifferentiation of podocytes in collapsing glomerulopathy due to HIV-1 infection[20, 21]. In the present study we evaluate the role of podocyte STAT3 on crescent formation by comparing the development of immune complex-mediated crescentic GN in mice with and without podocyte-specific STAT3 deletion.

Results

Mice with podocyte-specific deletion of STAT3

We generated a line of mice (Cre+;STAT3$^{f/f}$) with *Cre*-mediated deletion of a *Stat3* floxed allele (*Stat3*^{f})[22] driven by a podocyte-specific, 2.5-kb human *NPHS2* promoter[23]. To demonstrate that STAT3 deletion occurred in podocytes of Cre+;STAT3$^{f/f}$ mice we performed polymerase chain reaction to detect the presence of the wild-type, floxed, or

exon-18-to-20-deleted *Stat3* alleles (*Stat3*$^{+}$, *Stat3*^{f}, and *Stat*$^{\Delta}$, respectively) (Supp. Figure 1a and b). *Stat*$^{\Delta}$ was detected in the glomerular fraction (Glom), non-glomerular fraction (NGF) and the kidney cortex (Cortex) and completely absent in non-renal samples (i.e. Tail or Liver) (Supp. Figure 1c). Lower levels of Stat$^{\Delta}$ in NGF and Cortex compared to Glom reflect the minor amount of glomerular contamination in those samples. *Stat*$^{\Delta}$ was absent in glomeruli of Cre+;STAT3$^{+/+}$ mice, but present in both Cre+;STAT3$^{+/f}$ and Cre+;STAT3$^{f/f}$ mice (Supp. Figure 1d).

To compare the expression of podocyte STAT3 between Cre+;STAT3$^{f/f}$ and Cre +;STAT3$^{+/+}$ mice we performed co-immunolabeling of STAT3 and Wilm's Tumor (WT)-1, which is expressed by podocytes and parietal epithelial cells (PEC), but not by endothelial cells and mesangial cells. Since PECs can be distinguished from podocytes based on their localization within the glomerulus—PECs localize to the periphery and podocytes localize to center of the glomerulus—we examined STAT3 labeling of WT-1-positive nuclei near the center of glomerular tuft. We confirmed that STAT3 staining was nearly absent in WT-1-positive nuclei of Cre+;STAT3$^{f/f}$ mice (Figure 1a). To further confirm that podocyte STAT3 is reduced in Cre+;STAT3$^{f/f}$ mice we performed western blotting for total and Y7095-phosphorylated STAT3 (p-STAT3) on primary glomerular epithelial cells (PGEC) isolated from decapsulated glomeruli. Expression and phosphorylation of STAT3 were lower in PGECs of Cre+;STAT3$^{f/f}$ mice compared to Cre+;STAT3$^{+/+}$ mice (Figure 1b). *Stat3* mRNA transcript levels of PGECs from Cre+;STAT3$^{f/f}$ was 0.143±0.039 fold of Cre+;STAT3$^{+/+}$ (P<0.05, n=4 mice per group).

No significant difference in body or kidney weight was observed between Cre+;STAT3$^{+/+}$ and Cre+;STAT3$^{f/f}$ mice at 7 weeks of age (data not shown). Urinary albumin excretion as assessed by urinary albumin to creatinine ratio (UACR) was also not significantly different between Cre+;STAT3$^{+/+}$ and Cre+;STAT3$^{f/f}$ mice at 7 weeks of age (0.088±0.037 μg albumin/μg creatinine vs. 0.095±0.004 μg albumin/μg creatinine, n = 4 mice per group). Expression of a PEC-specific marker (claudin-1) and markers of differentiated podocytes (podocalyxin, WT-1, synaptopodin, and nephrin) was similar between the two groups of mice (Supp Figure 2). Ultrastructural examination of podocytes, podocyte foot processes, and PECs of Cre+;STAT3$^{f/f}$ mice (n = 2) did not reveal any obvious abnormalities (Figure 1c). The estimated number of WT-1 positive cells per μm^2 of glomerular tuft area was also not significantly different between Cre+;STAT3$^{+/+}$ and Cre+;STAT3$^{f/f}$ mice (4.2±0.6 *vs.* 4.1±0.5 nuclei per 1,000 μm^2 of glomerular tuft area, n = 3 mice per genotype).

Crescent formation and renal function of Cre+;STAT3$^{f/f}$ mice with crescentic GN

Nephrotic serum (NTS) enhanced crescents formation in both Cre+;STAT3$^{+/+}$ and Cre +;STAT3$^{f/f}$ mice compared to PBS-injected control mice of the same genotype 7 days after NTS injection (Figure 2a and b). However, NTS-injected Cre+;STAT3$^{+/+}$ mice developed significantly more crescents compared to NTS-injected Cre+;STAT3$^{f/f}$ mice (48.7 ± 3.2% *vs.* 14.2 ± 0.4% glomeruli with crescents, P<0.05, n = 4 mice per group). Urinary albumin to creatinine ratio (UACR), which is an indicator of urinary protein loss and renal injury, was significantly higher in the NTS-inject Cre+;STAT3$^{+/+}$ group compared to either PBS-injected Cre+;STAT3$^{+/+}$ or NTS-injected Cre+;STAT3$^{f/f}$ mice at 5 and 7 days after NTS

injection (Figure 2c, n = 4 mice per group). However, UACR was not significantly different between NTS- and PBS-injected Cre+;STAT3$^{f/f}$ mice. Serum levels of urea nitrogen and creatinine, which are markers of kidney function, were significantly higher in NTS-injected Cre+;STAT3$^{+/+}$ mice compared to PBS-injected Cre+;STAT3$^{+/+}$ and NTS-injected Cre+;STAT3$^{f/f}$ mice 7 days after NTS injection (Table 1, serum urea nitrogen: 72.4±5.4mg/dl *vs.* 21.5±0.3mg/dl and 32.1±1.7mg/dl, $P<0.05$, n = 4 per group; serum creatinine: 0.36±0.15mg/dl *vs.* 0.25±0.02mg/dl and 0.28±0.02mg/dl, $P<0.05$, n=4). Taken together these findings suggest that Cre+;STAT3$^{f/f}$ mice were protected from NTS-induced crescent formation and loss of renal function.

Proliferation and apoptosis of glomerular epithelial cells

Since STAT3 is known to drive podocyte de-differentiation and proliferation in HIVAN[20] and STAT3 activation has been observed in human kidney samples with crescentic GN[18, 19], here we examined the proliferation of podocytes and PECs in nephritic mice with and without podocyte STAT3 deletion. Staining for Ki-67, which is a marker of cell proliferation, showed that NTS injection increased the number of Ki-67-positive cells in glomeruli of both Cre+;STAT3$^{+/+}$ and Cre+;STAT3$^{f/f}$ mice compared to PBS injection of mice with the same genotype (Fig 3A and B, 13.1±0.96 *vs.* 1.1±0.44 Ki-67-positive nuclei/glom and 5.8±0.59 *vs.* 1.3±0.33 Ki-67-positive nuclei/glom, respectively, $P<0.05$, n = 4 mice per group). NTS-injected Cre+;STAT3$^{f/f}$ mice, however, had significantly less Ki-67 positive nuclei compared to NTS-injected Cre+;STAT3$^{+/+}$ mice (5.8±0.59 *vs.* 13.1±0.96 Ki-67-positive nuclei/glom, $P<0.05$, n=4 mice per group). To determine whether podocyte STAT3 deletion had an impact on apoptosis of glomerular cells we performed TUNEL assay. No TUNEL positive cells was observed in PBS-injected Cre+;STAT3$^{+/+}$ and Cre+;STAT3$^{f/f}$ mice (30 glomeruli were examined per mouse, n = 3 mice per group). For NTS-injected mice, TUNEL-positive cells were present in crescentic glomeruli of both NTS-injected Cre+;STAT3$^{+/+}$ and Cre+;STAT3$^{f/f}$ mice (Figure 3c). The number of TUNEL-positive cells within crescentic glomeruli was not significantly different between NTS-injected Cre+;STAT3$^{+/+}$ and Cre+;STAT3$^{f/f}$ mice (0.32±0.10 vs. 0.37±0.11 cells per crescentic glomeruli, 20 crescentic glomeruli per mouse, n = 3 mice per group, Figure 3d). This suggests that reduced crescent formation in the NTS-injected Cre+;STAT3$^{f/f}$ group was not due to a difference in apoptosis of glomerular cells. To ensure the TUNEL assay was sufficiently sensitive to detect apoptotic cells, we also included a kidney section of a mouse with transgenic overexpression of HIV-1 genes, which exhibits prominent tubular cell apoptosis[24].

Cellular composition of glomerular crescents

To determine whether deletion of podocyte STAT3 altered the cellular composition of glomerular crescents we performed immunolabeling of kidney sections for podocyte, PEC, and macrophage markers. Staining for podocyte markers—nephrin and synaptopodin—were more prominent in both of the PBS-injected control groups compared to NTS-injected Cre+;STAT3$^{+/+}$ mice, but not different from NTS-injected Cre+;STAT3$^{f/f}$ mice (Figure 4a). Similarly, glomerular mRNA transcripts of both nephrin and synaptopodin in NTS-injected Cre+;STAT3$^{+/+}$ mice were significantly less compared to NTS-injected Cre+;STAT3$^{f/f}$ mice and PBS-injected Cre+;STAT3$^{+/+}$ mice (Figure 4c). A lower nephrin and synaptopodin

expression could be from either downregulation of gene expression in injured and dedifferentiated podocytes[25, 26] or reduction of podocyte number. To determine whether STAT3 deletion alters the recruitment of podocytes in crescents we also performed immunostaining for nestin (Figure 4c). Nestin is an intermediate filament expressed by podocytes; and nestin expression in podocytes is preserved in crescentic GN[27]. We found that more nestin staining localized to the periphery of crescentic glomeruli (Figure 4c) compared to non-crescentic glomeruli, which is consistent with previous observation[27]. The intensity of glomerular nestin staining, however, was not different between NTS-injected Cre+;STAT3$^{+/+}$ and Cre+;STAT3$^{f/f}$ mice, suggesting that the difference in nephrin and synaptopodin expression between the two NTS-injected groups was not due to a change in the amount of podocytes.

To assess whether podocyte STAT3 deletion had an effect on PEC accumulation we performed immunostaining for claudin-1, which is expressed by PECs[14]. Claudin-1 staining localized to the periphery of glomeruli in all four groups of mice (Figure 4d and e). Focal accumulation of claudin-1-positive cells was observed within crescents of NTS-injected mice (arrows in Figure 4d). Co-immunostaining of F4/80, which is an extracellular macrophage membrane marker, with claudin-1 revealed a pattern of F4/80 staining that surrounded the glomerulus without intra-glomerular involvement (Figure 4d), suggesting that macrophages do not contribute significantly to the cellular composition of crescents. When the percentage of glomerular area with claudin-1 staining was quantified by image analysis, a higher percentage of the area was claudin-1 positive in the NTS-injected Cre+;STAT3$^{+/+}$ than NTS-injected Cre+;STAT3$^{f/f}$ (Figure 4f, 8.1±2.3% *vs.* 3.4±0.7%, $P<0.001$, 30 glomeruli encompassing >100,000μm^2 per group were examined).

Glomerular deposition of immunoglobulin and C3 complement in GN

Deposition of heterologous antibody in the glomerulus is thought to cause glomerular injury directly by antibody-mediated injury of glomerular cells and indirectly by leukocyte recruitment with subsequent leukocyte-mediated tissue injury[28]. To understand why Cre+;STAT3$^{f/f}$ mice were protected against the development crescentic GN we examined the glomerular deposition of mouse immunoglobulin (Ig)G, sheep IgG and C3 complement. Cre+;STAT3$^{f/f}$ and Cre+;STAT3$^{+/+}$ mice injected with NTS displayed a similar pattern and intensity of staining for mouse IgG, sheep IgG, and C3 complement (Figure 5a, b, and c), suggesting that protection against crescent formation in Cre+;STAT3$^{f/f}$ mice was not due to a reduction in immune complex deposition.

STAT3 activation and target gene expression in GN

Next, we examined STAT3 activation in glomeruli of nephritic mice with and without podocyte STAT3 deletion by immunostaining for phospho-STAT3 (Y705). Phospho-STAT3 staining was more pronounced in NTS-injected Cre+;STAT3$^{+/+}$ mice compared to PBS-injected Cre+;STAT3$^{+/+}$ mice and NTS-injected Cre+;STAT3$^{f/f}$ mice (Figure 6a). Phospho-STAT3 staining localized to cells lining Bowman's capsule and within cellular crescents. Since STAT3 mediates pro-inflammatory gene expression, we also compared the mRNA transcript levels of STAT3 target genes involved in inflammatory response (interleukin 6, *Il-6*) and expressed at sites of injury (inter-cellular adhesion molecule-1, *Icam1* and

chemokine C-C motif ligand 2, *Ccl2*). Glomerular mRNA expressions of *Icam1*, *Ccl2*, and *Il6* were significantly higher in NTS-injected Cre+;STAT3$^{+/+}$ compared to NTS-injected Cre+;STAT3$^{f/f}$ mice and to PBS-injected Cre+;STAT3$^{+/+}$ mice (Figure 6b), suggesting deletion of podocyte STAT3 abrogates NTS-induced expression of pro-inflammatory target genes in the glomerulus. Glomerular expression of other STAT3 target genes, such as *Socs3*, *Vegf*, *Ccl5*, and *Bclx*, were not significantly different between NTS-injected Cre+;STAT3$^{+/+}$ mice and NTS-injected Cre+;STAT3$^{f/f}$ mice (data not shown).

STAT3 activation and target gene expression in STAT3-deleted podocytes

Since glomeruli contain podocytes as well as other cell types (i.e. endothelial cells, mesangial cells and PECs) and podocytes constitute only a small fraction of the total cell mass in the glomerulus, it is not possible to determine gene expression in podocytes from isolated glomerular samples. To delineate podocyte-specific response we used conditionally immortalized murine podocytes as well as PGECs isolated from Cre+;STAT3$^{+/+}$ and Cre +;STAT3$^{f/f}$ mice. The classic pathway of STAT3 signaling begins with ligand-mediated activation of gp130 receptor and epidermal growth factor (EGF) receptor by IL-6/IL-10 and EGF, respectively. To examine whether IL-6 and EGF could activate STAT3 signaling in podocytes we exposed cultured murine podocytes to IL-6 and EGF and then performed western blotting to determine STAT3 phosphorylation, which is a marker of activation of STAT3 signaling. Ten ng/ml of either IL-6 or EGF increased STAT3 phosphorylation (Y705) in a time-dependent manner with peak STAT3 phosphorylation occurring at 30mins and at 10mins, respectively (Figure 7a and b). Pretreatment with a specific kinase inhibitor of EGF receptor (EGFR), AG1478, prevented EGF-induced STAT3 phosphorylation (Figure 7b), suggesting that EGF-induced STAT3 activation in podocytes occurred in an EGFR-dependent manner. Effects of IL-6 and EGF on STAT3 phosphorylation and expression were further confirmed in PGECs: Both EGF (1ng/ml and 10ng/ml for 10min) and IL-6 (10ng/ml for 30min) treatments enhanced STAT3 phosphorylation in Cre+;STAT3$^{+/+}$ PGECs, but not in Cre+;STAT3$^{f/f}$ PGECs (Figure 7c). The basal level of phospho-STAT3 was different between cultured podocyte cell line and PGECs, which could be explained by a low basal expression of temperature-sensitive T-antigen in the cultured podocytes, which are conditionally immortalized. We also determined the effect of IL-6 on STAT3 target gene expression and found that IL-6 treatment significantly increased the expression of *Icam1, Ccl2, Il6 and Socs3* in Cre+;STAT3$^{+/+}$ PGECs, but not in Cre+;STAT3$^{f/f}$ PGECs (Figure 7d).

Discussion

To our knowledge this is the first study to establish a functional role for podocyte STAT3 activation in crescentic GN. We found that podocyte-specific STAT3 deletion attenuates NTS-induced crescent formation and renal injury. Our results suggest that STAT3 deletion reduces crescent formation by preventing recruitment of PECs and downregulation of podocyte differentiation markers. We postulate that podocyte STAT3 deletion could have attenuated crescent formation through one of three potential mechanisms: 1) STAT3 deletion mitigates the podocyte's response to injury; 2) STAT3 deletion disrupts a potential paracrine signaling pathway between podocyte and PEC to prevent PEC proliferation; and

3) STAT3 deletion modulates the innate immune response of podocytes, which drives injury in many forms of GN[1].

Even though podocyte is thought to be the initial target of injury that triggers crescent formation and immune complex-mediated GN, it remains to be determined how podocyte injury leads to accumulation of PECs. Interestingly, specific ablation of podocytes in several experimental models—where podocytes express exogenous receptors that trigger cell death in the presence of a cognate receptor ligand—has consistently resulted in segmental glomerulosclerosis without glomerular epithelial cell proliferation[29–31]. However, it is important to note that not all insults directed to the podocyte lead to glomerulosclerosis. For instance, podocyte-specific deletion of *Vhlh*[11] and expression of HIV-1 genes[15] have shown to trigger glomerular epithelial cell proliferation. More recently, subtotal ablation of PECs was found to cause activation of PEC and crescent formation[16]. We suspect the response (glomerulosclerosis vs. proliferation) of glomerular epithelial cells to podocyte-specific injury is likely dependent upon the nature of the initial insult/stimulus on podocytes.

In our model, podocyte STAT3 deletion altered the podocyte's response to IL-6 and EGF. IL-6 increased the expression of STAT3 target genes (*Icam1, Ccl2, Il6* and *Socs3*) in PGECs; this effect was abrogated in podocytes with STAT3 deletion. Although we did not directly measure the production of IL-6 and EGF in NTS-induced GN, autocrine signaling of EGF through EGFR in the podocyte has already been shown to promote glomerular injury and renal failure in human with GN and the NTS model of GN[32] and podocytes are known to express IL-6[33]. We speculate that IL-6 and EGF could be produced by intrinsic glomerular cells (podocytes, mesangial cells and endothelial cells) and circulating immune cells recruited to the glomeruli (lymphocytes). Localized accumulation of IL-6 and EGF in the injured glomerulus could then activate JAK/STAT signaling in the podocyte (as depicted in Figure 7e). Consistent with this supposition, urinary IL-6 is higher in patients advanced lupus nephritis[34] and a case of anti-neutrophil cytoplasmic antibody-associated crescentic GN has been successfully treated using humanized anti-IL-6 receptor antibody[35]. Furthermore, mice treated with an EGF receptor (EGFR) inhibitor or deficient of EGFR in the podocyte are protected from NTS-induced renal failure and GN[32]. Since abrogation of STAT3 signaling in the podocyte prevented the recruitment of PECs in our model, we suspect STAT3 mediates a potential podocyte-to-PEC crosstalk.

In our murine model, *NPHS2* promoter drove STAT3 deletion in podocytes. Although *NPHS2* is normally expressed in podocytes, we cannot completely exclude the possibility that *NPHS2* expression could be altered in glomerular disease. Nevertheless, it is reassuring to note that several other studies have used *NPHS2*-Cre mice in the setting of NTS-induced GN[32, 36] without reports of aberrant *NPHS2* expression contributing to inappropriate *Cre* recombination. Deletion of podocyte STAT3 was not complete when driven by the NPHS2 promoter, which is another limitation of our model. Since crescent formation was not completely prevented in NTS-injected Cre+;STAT3$^{f/f}$ mice, it is not possible for us to deduce whether the lack of complete protection from crescent formation was due to incomplete STAT3 deletion or other nephritogenic mechanisms independent of STAT3 activation. Nonetheless, nephritic Cre+;STAT3$^{f/f}$ mice had significantly less crescent

formation and renal failure compared to nephritic mice without STAT3 deletion. These results suggest podocyte STAT3 has a key role in the development of crescentic GN.

There was a trend for increased glomerular synaptopodin expression in the Cre+;STAT3$^{f/f}$ group, which did not attain statistical significance. When we examined the promoter region of *Synpo* for STAT3 binding sites using a database of predicted transcription factor binding sites (SABiosciences, DECODE database), only one predicted STAT3 binding site (TTCCTGGAA; at chr18:60792618-60792626) located ~168kb upstream of the *Synpo* transcription start site (TSS) was identified. This STAT3 binding site is likely too distant from the TSS to regulate transcription of *Synpo*. It is also possible that STAT3 could regulate *Synpo* expression independent of transcription of *Synpo*. While there is a trend towards higher *Synpo* expression, it is reassuring that expression of other podocyte markers (i.e. nephrin, nestin, and WT1) in the Cre+;STAT3$^{f/f}$ group was not different from the Cre +;STAT3$^{+/+}$ group at baseline.

In conclusion, we demonstrated that podocyte STAT3 activation is important for crescent formation and development of renal failure in NTS-induced GN. We also identified a role for podocyte STAT3 in the recruitment of PECs and expression of STAT3 pro-inflammatory target genes in a murine model of crescentic GN.

Methods

Animal husbandry and genotyping

To generate mice with podocyte-specific deletion of STAT3, a mouse homozygous for a STAT3 allele with *lox*P sites flanking exons 18, 19 and 20 (*Stat3^{f}*)[22] was crossed to a mouse with podocyte-specific expression of the *Cre* recombinase[23]. Both mice were on the C57Bl6 background. Subsequent crossings of F1 progenies that were positive for the *Cre* transgene and heterozygous for the *Stat3^{f}* allele (Cre+;STAT3$^{f/+}$) generated Cre+;STAT3$^{+/+}$, Cre +;STAT3$^{f/+}$, and Cre+;STAT3$^{f/f}$ mice. Mice of all three genotypes were born at expected Mendelian ratio and appeared healthy and fertile. Four to six male mice of each genotype were used for the study. Primers 1 (5′-ATT GGA ACC TGG GAC CAA GTG G-3′) and 2 (5′-ACA TGT ACT TAC AGG GTG TGT GC-3′) were used for genotyping to detect a 520-bp band for the *Stat3^{f}* allele and a 480-bp band for the wild type (*Stat3^{+}*) allele. Primers 1 and 3 (5′-GCT GGC TCA TAG GCA AAA ACA C-3′) were used to detect the *Stat$^{\Delta}$* allele (480-bp band). Thermoprofile for the PCR reaction was as follows: 95°C for 2min followed by 30 cycles of 95°C for 30s, 58.7°C for 1min and 72°C for 1min, then 72°C for 5min. Studies were performed in accordance with the guidelines of and approved by the Institutional Animal Care and Use Committee at the Mount Sinai School of Medicine.

Induction of glomerulonephritis

Male mice at 7 weeks of age were sensitized with intraperitoneal injection of 0.5mg sheep IgG with complete Freund's adjuvant or normal saline as control. Six days later, animals were injected with either 100μl of NTS, which was diluted to 66.7g/L in sterile phosphate buffer solution (PBS)[37], or PBS alone as a control *via* the tail vein. Urine samples were collected daily when possible and at the termination of the experiment. Seven days after

NTS injection, mice were killed and serum samples collected. Kidneys were saved for histology, protein, total RNA, and glomeruli extraction.

Measurements of serum urea nitrogen and creatinine

Serum samples were collected after centrifugation and stored at −80°C until measurement. Serum urea nitrogen content was measured using a commercially available kit (Bioassay Systems, Hayward, CA). Whole blood samples were allowed to sit at room temperature for 30min prior to centrifugation at 14,000rpm for 10mins. Serum creatinine was measured by a high performance liquid chromatography (HPLC)-based method following a previously published protocol[38] with some modifications: five microliters of serum per mouse was processed as described and then assayed using a Shimadzu Prominence HPLC unit connected with a Hamilton cation exchange column (PRP-X200).

Measurement of urinary albumin excretion

To quantify proteinuria we measured urine creatinine and urine albumin concentration to calculate UACR. Urine albumin was quantified using an ELISA kit (Bethyl Laboratory, Houston, TX). Urine creatinine was measured in the same urine sample as urine albumin using QuantiChrom Creatinine Assay Kit (DICT-500, Bioassay Systems).

Podocyte Cell culture

A cell line of conditionally immortalized murine podocytes was cultured as described[39]. Cells were grown in RPMI-1640 medium supplemented with fetal bovine serum (FBS, final concentration 10%) and penicillin-streptomycin antibiotics (final concentration 1%). Cells were cultured on rat tail collagen-I-coated plates and maintained at 33°C (5% CO_2, 90% humidity). Prior to experiments, cells were moved to a 37°C incubator and cultured for at least 7 days.

Glomerular isolation and primary glomerular epithelial cell culture

Glomeruli from mice were isolated by perfusion of magnetic particles as described[40] with some minor modifications. For isolation of PGECs, all procedures were performed in a ventilated dissection hood under clean contaminated condition. Tosylated M450 Dynabeads beads (Invitrogen) were inactivated and then diluted in 30ml of 1xHBSS, pH 7.1 with 1%BSA for perfusion of mice through the left ventricle of the heart (5×10^7 beads/mouse). Iliac vein below the kidney was punctured immediately before perfusion. After perfusion, both kidneys were removed, cut into ~1mm^3 pieces and then digested in a digestion buffer containing 1mg/ml of collagenase A and 100U/ml of DNaseI for 30min at 37°C. After digestion, samples were passed through 100μm cell strainers and washed with ice-cold 1x HBSS, pH7.1. Washed cells were centrifuged for 5min at 200g and supernatant were aspirated and discarded. Cell pellet was re-suspended in HBSS and glomeruli containing magnetic Dynabeads were collected using a magnetic particle concentrator. An aliquot (1:1,500) of the glomerular isolate was visualized under a microscope to ensure that the sample contained <5 tubular fragments per 200x field. Majority of the isolated glomeruli (>80%) were decapsulated—similar to what had been reported previously[40]. Isolated glomeruli were transferred onto a 6-cm tissue culture dish coated with type I collagen and

cultured in RPMI1640 medium supplemented with 10%FBS and 1% Pen/Strep. Glomeruli and cells were allowed to attach to the plate for 5 days in a 37°C incubator without any agitation. Five days later, glomeruli and outgrowth cells were detached from the plate using a 0.12% trypsin-EDTA solution. Trypsinized cells were strained pass a 40μm cell strainer and re-plated onto collagen-coated dishes. More than 80% of the filtered cells were podocalyxin-positive when examined by immunostaining (data not shown). These cells (PGECs) were allowed to grow to 80% confluence before passaging at a ratio of 1:3. PGECs passaged less than 3 times were used in our experiments. For experiments on interleukin-6 (IL6)-induced expression of STAT3 target genes, PGECs from two mice per group were pooled.

Antibodies and reagents

Antibodies to phospho-STAT3 (Y705) and to total STAT3 were purchased from Cell Signaling (Danvers, MA), rabbit antibody to Wilm's Tumor 1 (WT-1) from Novus Biologicals (Littleton, CO), rabbit antibody to Ki-67 from Vector Laboratories (Burlingame, CA), antibody to actin from Sigma Aldrich (St. Louis, MO), rabbit antibody to nephrin was a gift from Dr. Lawrence Holzman (University of Pennsylvania, PA), rabbit antibody to claudin-1 and rat antibody to F4/80 from eBioscience, rabbit antibody to nestin from Santa Cruz Biotechnology, rabbit antibody to synaptopodin antibody was a gift from Dr. Peter Mundel (Massachusetts General Hospital, Boston, MA), antibodies to mouse IgG and to sheep IgG from Jackson ImmunoResearch Laboratories (West Grove, PA), and FITC-labeled antibody to mouse complement component C3 from Cedarlane Labs. IL-6 was purchased from Sigma Aldrich, EGF from R&D Systems (Minneapolis, Minnesota), and AG1478 from Fisher Scientific.

Real-time PCR

Samples were stored in RNAlater (Qiagen) solution at −80°C until processing. Total RNA was extracted from isolated glomeruli or cultured podocytes using RNeasy Mini Kit (Qiagen). Superscript III First-Strand Synthesis SuperMix (Invitrogen) was used for reverse transcription of 1μg of total RNA. PCR was performed using Sybr Green Master Mix (Applied Biosystems) and the Applied Biosystems 7500 Real-time PCR system. Quantitative RT-PCR for gene expression was performed using cDNA reverse transcribed from total RNA extracted from isolated glomeruli, PGECs, or podocyte cell line using primers corresponding to the gene of interest (Table 1). For each gene target, three RT-PCR reactions were performed (technical replicates). Ct values of the gene targets were normalized to GAPDH. Fold change in expression of target genes compared to the reference group was calculated using the $2^{-\Delta\Delta CT}$ method with GAPDH as the calibrator. PCR primers were designed using Primer-Blast (NCBI) to span at least one intron of the targeted gene (See Table 2). To study IL-6 induced STAT3 target gene expression, PGECs were treated with and without IL-6 three times (biological replicates).

Western blot analysis

Western blotting was performed using 60μg of protein lysate per lane under denaturing condition. Cells were serum starved for 16h before treatment with PBS, EGF, IL-6, or AG1478 for the indicated amount of time prior to protein extraction.

Histopathology and immunohistochemistry of mouse tissue

Kidney samples were either frozen in optimal cutting temperature compound or fixed in 10% formalin and then embedded in paraffin. Periodic Acid Schiff's staining of paraffin-sections was used for quantification of crescents. The percentage of glomeruli with crescent formation was determined by an examiner masked to the experimental condition. At least 30 glomeruli per animal were counted. Each biological group included 4 mice. Paraffin-embedded sections were used for pSTAT3 and Ki-67 staining as described. For quantification of Ki-67-positive nuclei, 15 glomeruli per mice and four mice from each group were examined to calculate the number of stained nuclei.

Immunofluorescence labeling and microscopy

Frozen sections of kidneys were used for podocalyxin, nephrin, synaptopodin, WT-1, nestin, claudin-1, F4/80, mouse IgG, sheep IgG, and C3 complement staining. Stained sections were visualized and imaged were acquired using Zeiss Axioplan2 IE (Carl Zeiss Microscopy). ImageJ[41] was used to quantify podocalyxin, nephrin and synaptopodin staining intensity and the percentage of glomerular area with claudin-1 labeling. For assessment of podocalyxin, nephrin, and synaptopodin staining, 10 to 20 glomeruli from 3 mice of each biological group were measured. For quantification of glomerular claudin-1 labeling, thirty glomeruli encompassing more than 100,000μm^2 of glomerular area were assessed for each biological group. To estimating WT-1 cell number in glomerular tuft we performed WT-1 staining on perfusion-fixed, frozen kidney samples sectioned at 6μm. Digitized images at 400x magnification were taken. The number of WT-1-positive nuclei in a glomerular tuft was counted and the area of the glomerular tuft was measured using ImageJ. The number of WT-1 nuclei per μm^2 of glomerular tuft area was calculated and then averaged. Twenty glomeruli were examined per mouse and 3 mice per group were assessed.

TUNEL assay

DeadEnd Colometric TUNEL System from Promega (Madison, WI) was used to detect apoptic cells on formalin-fixed, paraffin-embedded kidney sections. Manufacturer's protocol was used to processes the sections. For PBS-injected groups, 30 glomeruli per mouse and 3 mice per group were examined. For NTS-injected groups, 20 glomeruli with crescent involvement and 3 mice per group were examined. As a positive control for the TUNEL assay, kidney sections of mice with transgenic overexpression of HIV-1 genes were also examined.

Transmission electron microscopy

Kidney cortex samples fixed in 2.5% glutaradehyde were sectioned, mounted on a copper grid, and then images were photographed using a Hitachi H7650 microscope (Tokyo, Japan) as previously described[42].

Statistical analysis

Data are expressed as mean ± s.e.m. Statistical analyses were performed using GraphPad Prism. For comparison of means between groups, one-way analysis of variance was performed followed by Tukey post-test using significance cut off of < 0.05.

Supplementary Material

Refer to Web version on PubMed Central for supplementary material.

Acknowledgments

Source of Support: NIH 1R01DK078897, NIH 5K08DK082760, NIH1R01DK088541-01A1 and Veterans Affairs Merit Review Award 1I01BX000345.

We would like to thank Pete Mundel (Massachusetts General Hospital, Boston) for sharing cultured conditionally immortalized podocytes. JCH is supported by NIH 1R01DK078897 and 1R01DK088541-01A1 and a Veterans Affairs Merit Review Award 1I01BX000345; PYC is supported by NIH 5K08DK082760.

References

1. Couser WG. Basic and translational concepts of immune-mediated glomerular diseases. Journal of the American Society of Nephrology : JASN. 2012; 23:381–399. [PubMed: 22282593]
2. Detwiler RK, Falk RJ, Hogan SL, et al. Collapsing glomerulopathy: a clinically and pathologically distinct variant of focal segmental glomerulosclerosis. Kidney international. 1994; 45:1416–1424. [PubMed: 8072254]
3. Moudgil A, Nast CC, Bagga A, et al. Association of parvovirus B19 infection with idiopathic collapsing glomerulopathy. Kidney international. 2001; 59:2126–2133. [PubMed: 11380814]
4. Li RM, Branton MH, Tanawattanacharoen S, et al. Molecular identification of SV40 infection in human subjects and possible association with kidney disease. Journal of the American Society of Nephrology : JASN. 2002; 13:2320–2330. [PubMed: 12191976]
5. Markowitz GS, Appel GB, Fine PL, et al. Collapsing focal segmental glomerulosclerosis following treatment with high-dose pamidronate. Journal of the American Society of Nephrology : JASN. 2001; 12:1164–1172. [PubMed: 11373339]
6. Stokes MB, Davis CL, Alpers CE. Collapsing glomerulopathy in renal allografts: a morphological pattern with diverse clinicopathologic associations. American journal of kidney diseases : the official journal of the National Kidney Foundation. 1999; 33:658–666. [PubMed: 10196006]
7. Couser WG. Glomerulonephritis. Lancet. 1999; 353:1509–1515. [PubMed: 10232333]
8. Albaqumi M, Barisoni L. Current views on collapsing glomerulopathy. Journal of the American Society of Nephrology : JASN. 2008; 19:1276–1281. [PubMed: 18287560]
9. Jennette JC. Rapidly progressive crescentic glomerulonephritis. Kidney international. 2003; 63:1164–1177. [PubMed: 12631105]
10. Moeller MJ, Soofi A, Hartmann I, et al. Podocytes populate cellular crescents in a murine model of inflammatory glomerulonephritis. Journal of the American Society of Nephrology : JASN. 2004; 15:61–67. [PubMed: 14694158]
11. Ding M, Cui S, Li C, et al. Loss of the tumor suppressor Vhlh leads to upregulation of Cxcr4 and rapidly progressive glomerulonephritis in mice. Nature medicine. 2006; 12:1081–1087.
12. Bariety J, Bruneval P, Meyrier A, et al. Podocyte involvement in human immune crescentic glomerulonephritis. Kidney international. 2005; 68:1109–1119. [PubMed: 16105041]
13. Smeets B, Angelotti ML, Rizzo P, et al. Renal progenitor cells contribute to hyperplastic lesions of podocytopathies and crescentic glomerulonephritis. Journal of the American Society of Nephrology : JASN. 2009; 20:2593–2603. [PubMed: 19875807]
14. Smeets B, Uhlig S, Fuss A, et al. Tracing the origin of glomerular extracapillary lesions from parietal epithelial cells. Journal of the American Society of Nephrology : JASN. 2009; 20:2604–2615. [PubMed: 19917779]
15. Zhong J, Zuo Y, Ma J, et al. Expression of HIV-1 genes in podocytes alone can lead to the full spectrum of HIV-1-associated nephropathy. Kidney international. 2005; 68:1048–1060. [PubMed: 16105035]

16. Sicking EM, Fuss A, Uhlig S, et al. Subtotal ablation of parietal epithelial cells induces crescent formation. Journal of the American Society of Nephrology : JASN. 2012; 23:629–640. [PubMed: 22282596]
17. Yu H, Pardoll D, Jove R. STATs in cancer inflammation and immunity: a leading role for STAT3. Nat Rev Cancer. 2009; 9:798–809. [PubMed: 19851315]
18. Zhang W, Chen X, Shi S, et al. Expression and activation of STAT3 in chronic proliferative immune complex glomerulonephritis and the effect of fosinopril. Nephrol Dial Transplant. 2005; 20:892–901. [PubMed: 15755760]
19. Arakawa T, Masaki T, Hirai T, et al. Activation of signal transducer and activator of transcription 3 correlates with cell proliferation and renal injury in human glomerulonephritis. Nephrol Dial Transplant. 2008; 23:3418–3426. [PubMed: 18556750]
20. He JC, Husain M, Sunamoto M, et al. Nef stimulates proliferation of glomerular podocytes through activation of Src-dependent Stat3 and MAPK1,2 pathways. The Journal of clinical investigation. 2004; 114:643–651. [PubMed: 15343382]
21. Feng X, Lu TC, Chuang PY, et al. Reduction of Stat3 activity attenuates HIV-induced kidney injury. Journal of the American Society of Nephrology : JASN. 2009; 20:2138–2146. [PubMed: 19608706]
22. Jacoby JJ, Kalinowski A, Liu MG, et al. Cardiomyocyte-restricted knockout of STAT3 results in higher sensitivity to inflammation, cardiac fibrosis, and heart failure with advanced age. Proc Natl Acad Sci U S A. 2003; 100:12929–12934. [PubMed: 14566054]
23. Moeller MJ, Sanden SK, Soofi A, et al. Podocyte-specific expression of cre recombinase in transgenic mice. Genesis. 2003; 35:39–42. [PubMed: 12481297]
24. Bodi I, Abraham AA, Kimmel PL. Apoptosis in human immunodeficiency virus-associated nephropathy. American journal of kidney diseases : the official journal of the National Kidney Foundation. 1995; 26:286–291. [PubMed: 7645532]
25. Patrakka J, Tryggvason K. Nephrin--a unique structural and signaling protein of the kidney filter. Trends in molecular medicine. 2007; 13:396–403. [PubMed: 17766183]
26. Barisoni L, Bruggeman LA, Mundel P, et al. HIV-1 induces renal epithelial dedifferentiation in a transgenic model of HIV-associated nephropathy. Kidney international. 2000; 58:173–181. [PubMed: 10886562]
27. Thorner PS, Ho M, Eremina V, et al. Podocytes contribute to the formation of glomerular crescents. Journal of the American Society of Nephrology : JASN. 2008; 19:495–502. [PubMed: 18199804]
28. Salant D. Immune complex glomerulonephritis. Clinical and Experimental Nephrology. 1998; 2:271–275.
29. Wharram BL, Goyal M, Wiggins JE, et al. Podocyte depletion causes glomerulosclerosis: diphtheria toxin-induced podocyte depletion in rats expressing human diphtheria toxin receptor transgene. Journal of the American Society of Nephrology : JASN. 2005; 16:2941–2952. [PubMed: 16107576]
30. Matsusaka T, Xin J, Niwa S, et al. Genetic engineering of glomerular sclerosis in the mouse via control of onset and severity of podocyte-specific injury. Journal of the American Society of Nephrology : JASN. 2005; 16:1013–1023. [PubMed: 15758046]
31. Macary G, Rossert J, Bruneval P, et al. Transgenic mice expressing nitroreductase gene under the control of the podocin promoter: a new murine model of inductible glomerular injury. Virchows Archiv : an international journal of pathology. 2010; 456:325–337. [PubMed: 19806361]
32. Bollee G, Flamant M, Schordan S, et al. Epidermal growth factor receptor promotes glomerular injury and renal failure in rapidly progressive crescentic glomerulonephritis. Nature medicine. 2011
33. Xing CY, Saleem MA, Coward RJ, et al. Direct effects of dexamethasone on human podocytes. Kidney international. 2006; 70:1038–1045. [PubMed: 16837924]
34. Iwano M, Dohi K, Hirata E, et al. Urinary levels of IL-6 in patients with active lupus nephritis. Clin Nephrol. 1993; 40:16–21. [PubMed: 8358870]
35. Sumida K, Ubara Y, Suwabe T, et al. Complete remission of myeloperoxidase-anti-neutrophil cytoplasmic antibody-associated crescentic glomerulonephritis complicated with rheumatoid

arthritis using a humanized anti-interleukin 6 receptor antibody. Rheumatology (Oxford). 2011; 50:1928–1930. [PubMed: 21719417]

36. George B, Verma R, Soofi AA, et al. Crk1/2-dependent signaling is necessary for podocyte foot process spreading in mouse models of glomerular disease. The Journal of clinical investigation. 2012; 122:674–692. [PubMed: 22251701]
37. Salant DJ, Cybulsky AV. Experimental glomerulonephritis. Methods Enzymol. 1988; 162:421–461. [PubMed: 3265756]
38. Yuen PS, Dunn SR, Miyaji T, et al. A simplified method for HPLC determination of creatinine in mouse serum. American journal of physiology Renal physiology. 2004; 286:F1116–1119. [PubMed: 14970000]
39. Mundel P, Reiser J, Zuniga Mejia Borja A, et al. Rearrangements of the cytoskeleton and cell contacts induce process formation during differentiation of conditionally immortalized mouse podocyte cell lines. Exp Cell Res. 1997; 236:248–258. [PubMed: 9344605]
40. Takemoto M, Asker N, Gerhardt H, et al. A new method for large scale isolation of kidney glomeruli from mice. The American journal of pathology. 2002; 161:799–805. [PubMed: 12213707]
41. Schneider CA, Rasband WS, Eliceiri KW. NIH Image to ImageJ: 25 years of image analysis. Nature methods. 2012; 9:671–675. [PubMed: 22930834]
42. Mallipattu SK, Liu R, Zhong Y, et al. Expression of HIV transgene aggravates kidney injury in diabetic mice. Kidney international. 2013

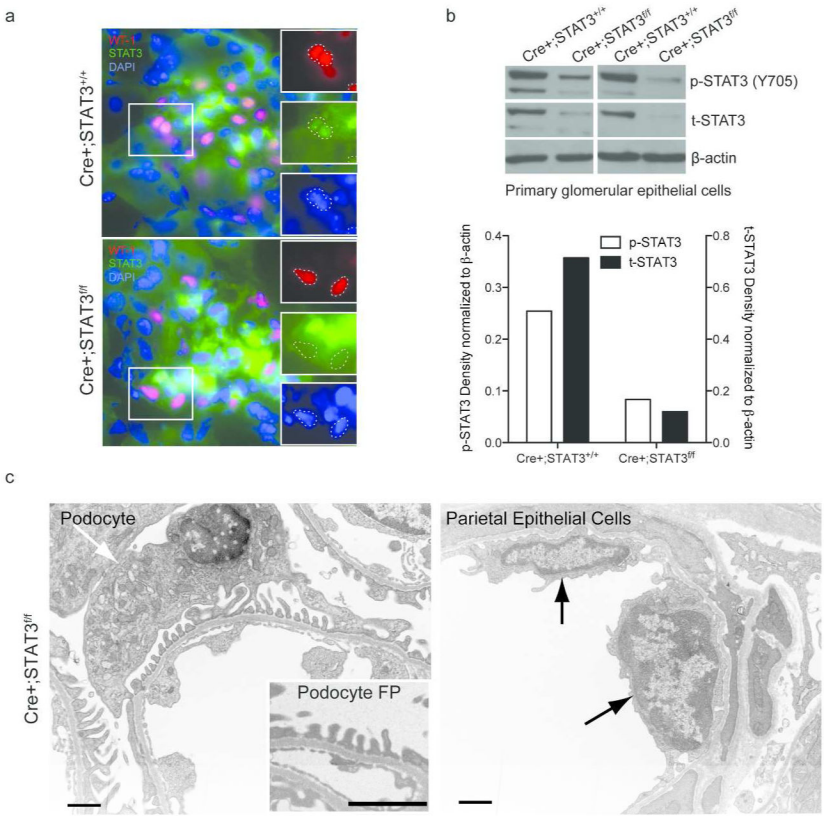

Figure 1.

Podocyte-specific deletion of STAT3. **a.** Co-immunolabeling of STAT3 and Wilm's Tumor 1 (WT-1). Insets correspond to WT-1 in red, STAT3 in green, and DAPI in blue for the area circumscribed by the box. Dashed lines circumscribe corresponding WT-1-positive regions of the inset panels. **b.** Western blots and a bar graph representing average band densitometry value corresponding to phospho (p)- and total (t)- STAT3 for primary glomerular epithelial cells isolated from Cre+;$STAT3^{+/+}$ and Cre+;$STAT3^{f/f}$ mice (n = 2 mice per genotype). **c.** Transmission electron micrographs of a podocyte (white arrow in left panel) and parietal epithelial cells (black arrows in right panel) for Cre+;$STAT3^{f/f}$ mice. Inset in the left panel: podocyte foot processes (FP). Scale Bar: 1μm.

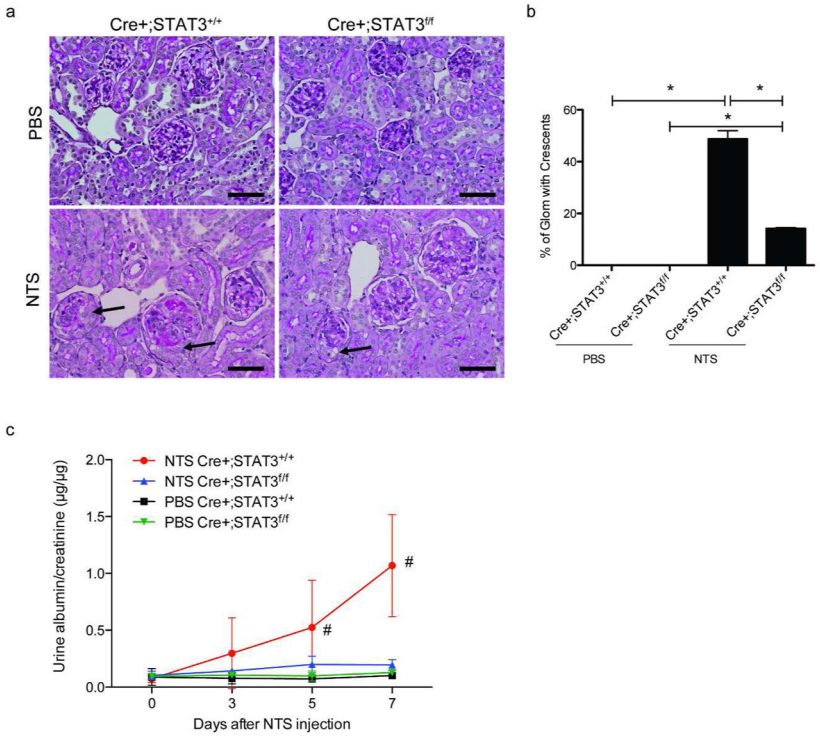

Figure 2.

Glomerular crescents and urinary protein excretion. **a.** Periodic acid Schiff staining of kidney sections 7d after nephrotoxic serum (NTS) or phosphate buffer solution (PBS) injection. Crescents within Bowman's space (arrows). Representative photographs are shown. Scale bar, 50μm. **b.** Bar graph summarizing the percentage of glomeruli with crescent involvement (30 glomeruli were assessed per mouse, n = 4 mice per group, **P*<0.05). **c.** Urine albumin to creatinine ratio of mice on day 0, 3, 5, and 7 after NTS injection. (n = 4 urine samples per time point, #*P*<0.05 compared to NTS Cre+;STAT3$^{f/f}$).

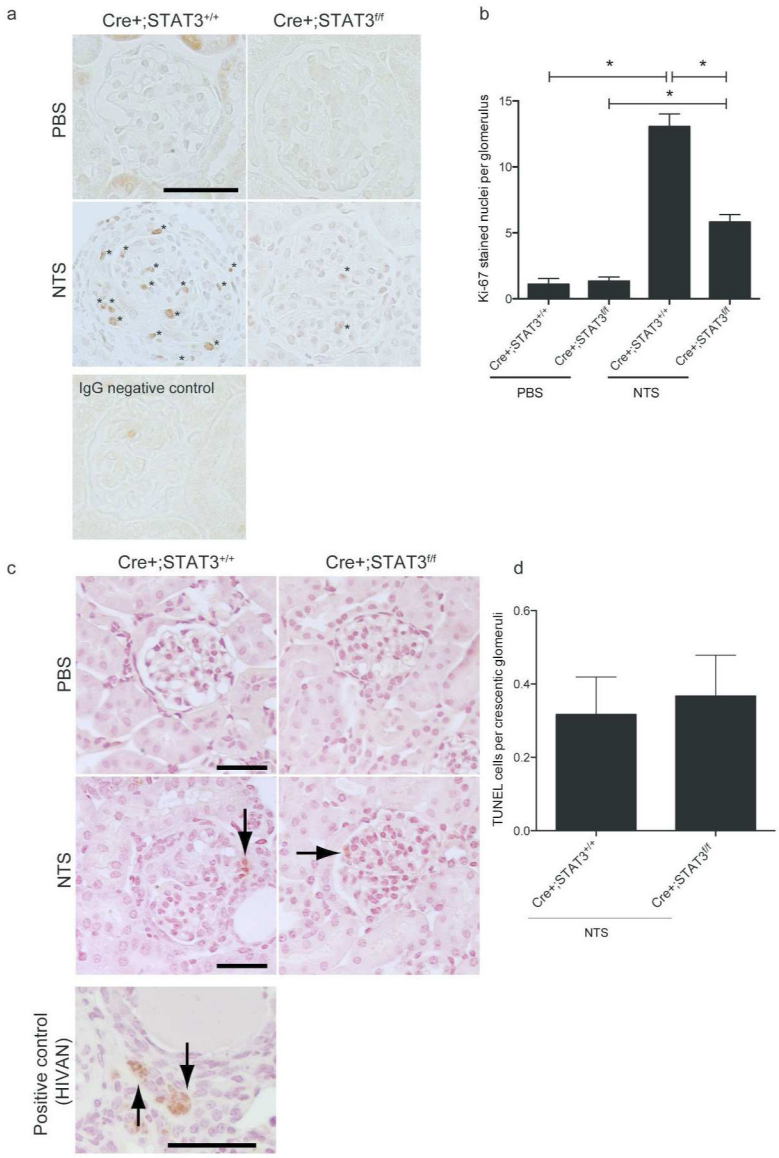

Figure 3.

Cell proliferation and apoptosis in crescentic GN. **a.** Immunostaining of Ki-67 in kidney sections. Ki-67-positive nuclei are marked with asterisks Representative pictures are shown. **b.** Bar graph summarizing quantitation of Ki-67 positive nuclei per glomerulus (n = 4 mice per group and 15 glomeruli were assessed per mouse. **P*<0.05). **c.** TUNEL assay of glomeruli of NTS or PBS injected mice. TUNEL staining of tubules from a mouse with expression of HIV-1 genes (positive control). **d.** Quantification of TUNEL positive cells per crescentic glomeruli.

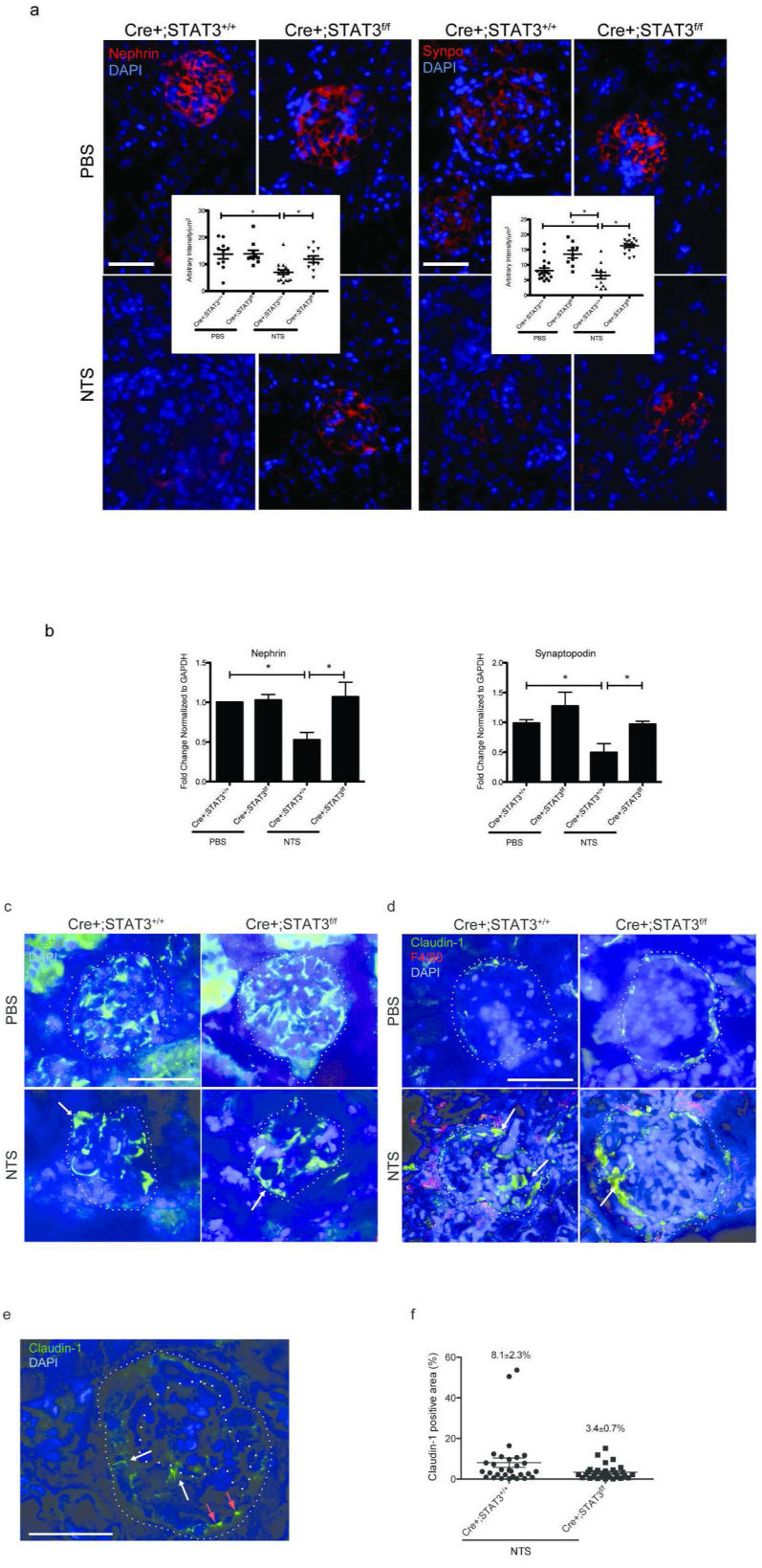

Figure 4.

Cellular composition of crescentic glomeruli. **a.** Immunofluorescence labeling for nephrin and synaptopodin. Nuclei are labeled by DAPI in blue. Inset graphs: Quantitative measurement of nephrin and synaptopodin (Synpo) staining per glomerular area is expressed as arbitrary intensity per μm^2 of glomerular area assessed (10 to 20 glomeruli from 2 mice per group were measured, $*P<0.05$). **b.** Quantitative real-time PCR for nephrin and synaptopodin mRNA expression was performed (n = 5 mice per group, $*P<0.05$). **c.** Immunofluorescence labeling of kidney section for nestin (green). Nestin staining near the periphery of glomeruli in NTS-injected groups (arrows). **d.** Co-immunolabeling of claudin-1 (green) and F4/80 (red). Accumulation of claudin-1 staining on the periphery of glomeruli (arrows). **e**. High magnification of a glomerulus with crescent involvement. Claudin-1 positive cells are present within the Bowman's capsule (red arrows) as well as within the glomerular crescent (white arrows). **f.** Percentage of glomerular area occupied by claudin-1 staining was quantified and results are displayed. Scale bars, 50μm. White dotted lines outline the glomeruli.

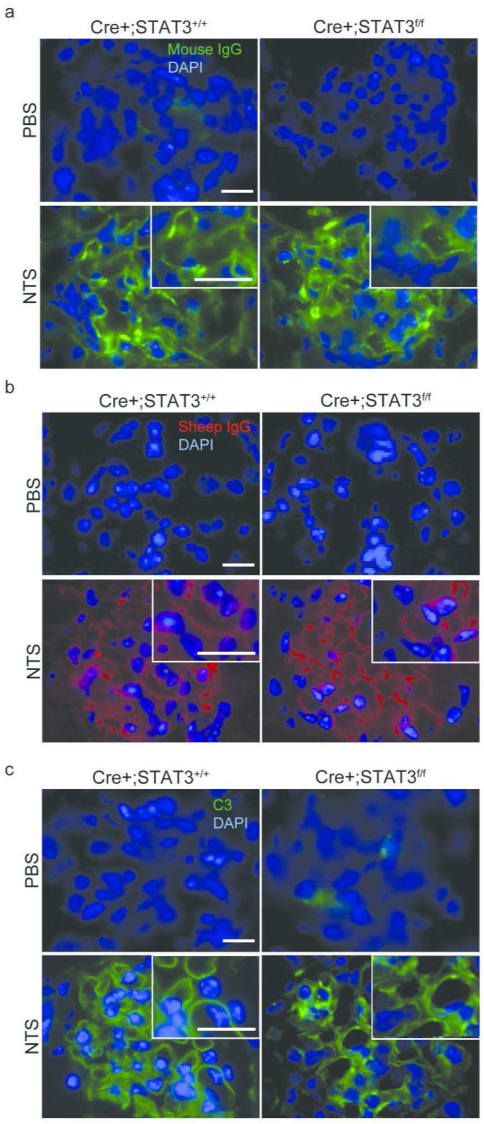

Figure 5.

Glomerular immune complex deposition. Immunofluorescence staining of kidney sections for mouse immunoglobulin (IgG) (**a**), sheep IgG (**b**), and C3 complement (**c**). Scale bar, 50μm. Insets are higher magnification views of glomerular capillary loops.

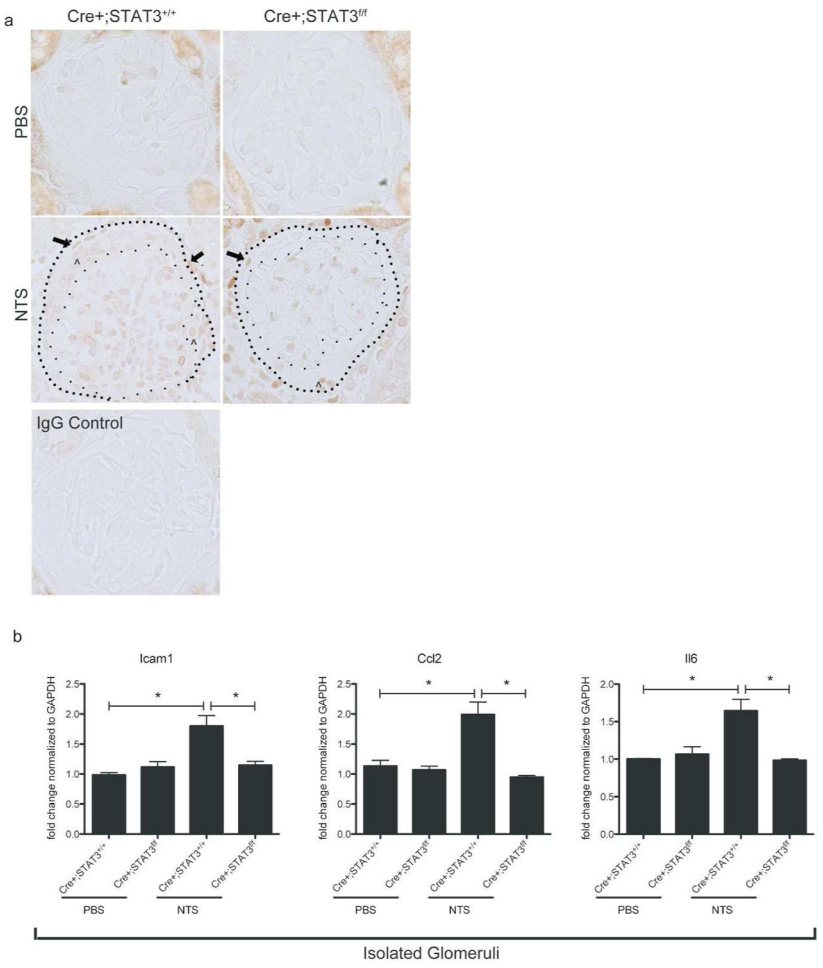

Figure 6.

STAT3 activation and target gene expression in the glomerulus. **a.** Phospho-STAT3 (p-STAT3) staining in kidney sections 7 days after NTS or PBS injection. Nuclear pattern of p-STAT3 staining of cells in crescents (^) and cells lining the Bowman's capsule (arrows) were noted. **b.** Glomerular expression of STAT3 target genes (*Icam1*, *Ccl2*, and *Il6*) was quantified by real-time PCR (**P*<0.05, n = 4 mice per group).

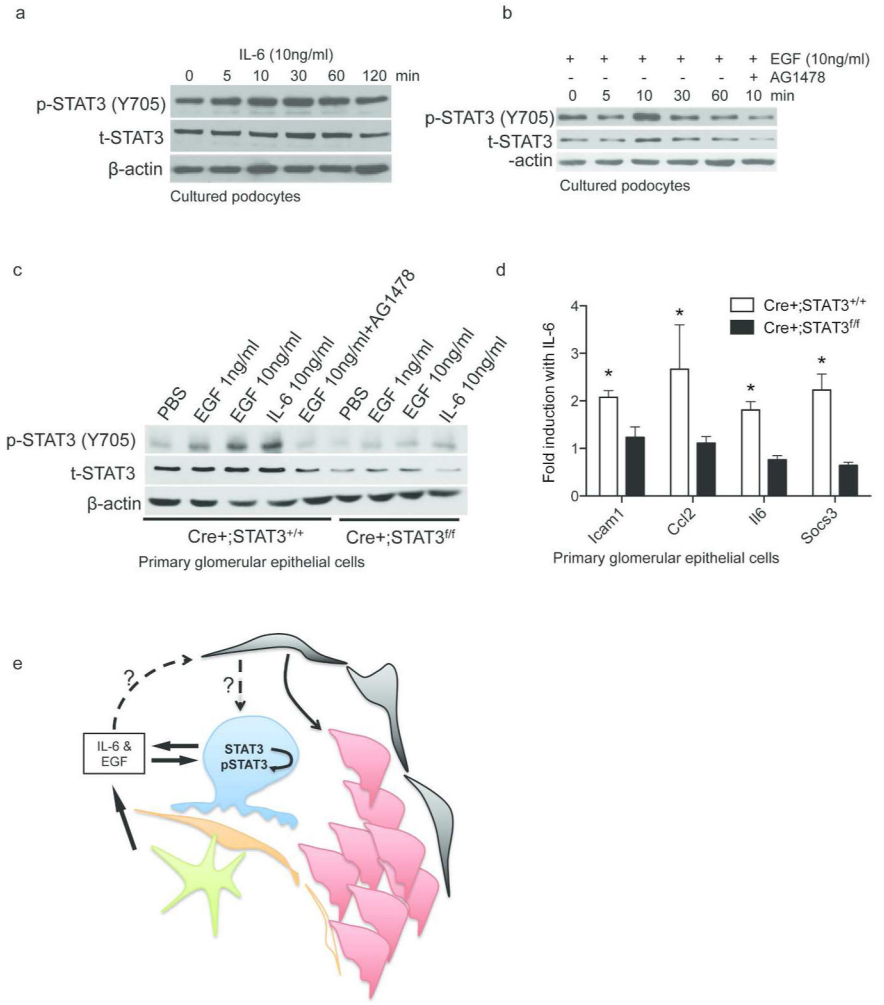

Figure 7.

Activation of STAT3 and expression of STAT3 target genes in podocytes. Western blots of phospho (p)- and total (t)- STAT3 and β-actin for conditionally immortalized murine podocytes treated with IL6 (10ng/ml) or EGF (10ng/ml) for 0, 5, 10, 30, 60, or 120 mins or EGF plus AG1478 for 10 mins (**a** and **b**). **c.** Western blots for primary glomerular epithelial cells (PGECs) isolated from Cre+;STAT3$^{+/+}$ and Cre+;STAT3$^{f/f}$ mice treated with PBS for 30mins, EGF (1ng, 10ng or 10ng with AG1478 pretreatment) for 10mins, or IL-6 (10ng/ml) for 30mins. **d.** Fold induction of STAT3 target gene expression (*Icam1*, *Ccl2*, *Il6*, and *Socs3*) in Cre+;STAT3$^{+/+}$ and Cre+;STAT3$^{f/f}$ PGECs treated with 10ng/ml of IL-6 (n = 3 biological replicates, **P*<0.05). **E.** Lymphocytes (green) and podocytes (blue) can produce IL-6 and EGF. IL-6 induces STAT3 phosphorylation and activation of STAT3 pathway in podocytes. STAT3 is required for IL-6-induced expression of pro-inflammatory STAT3 target genes and recruitment of parietal epithelial cells (red) in Bowman's space.

Table 1

Serum markers of kidney function: serum urea nitrogen and creatinine

Treatment groups	Serum urea nitrogen (mg dL^{-1})	Serum creatinine[#] (mg dL^{-1})
PBS Cre+;STAT3$^{+/+}$ (n= 4)	21.5 ± 0.3	0.25 ± 0.02
PBS Cre+;STAT3$^{f/f}$ (n= 4)	19.8 ± 0.7	0.27 ± 0.01
NTS Cre+;STAT3$^{+/+}$ (n= 4)	72.4 ± 5.4[a]	0.36 ± 0.15[c]
NTS Cre+;STAT3$^{f/f}$ (n= 4)	32.1 ± 1.7[b]	0.28 ± 0.02[d]

Serum samples obtained 7 days after NTS injection.

[#]Measured by an HPLC-based assay.

[a]$P<0.05$ compared to all other groups;

[b]$P<0.05$ compared to PBS Cre+;STAT3$^{f/f}$.

[c]$P<0.05$ compared to PBS Cre+;STAT3$^{+/+}$.

[d]$P<0.05$ compared to NTS Cre+;STAT3$^{+/+}$.

Table 2

Real Time PCR Primers

Gene	Forward	Reverse
Stat3	5′-CTACTGCGCTTCAGCGAGAGCAGC	5′-GTCTTCAGGTACGGGGCAGCAC
Ccl2	5′-TTAAAAACCTGGATCGGAACCAA	5′-GCATTAGCTTCAGATTTACGGGT
Icam1	5′-GTGATGCTCAGGTATCCATCCA	5′-CACAGTTCTCAAAGCACAGCG
Nphs1	5′-GTGCCCTGAAGGACCCTACT	5′-CCTGTGGATCCCTTTGACAT
Synpo	5′-GCCAGGGACCAGCCAGATA	5′-AGGAGCCCAGGCCTTCTCT
GAPDH	5′-GCCATCAACGACCCCTTCAT	5′-ATGATGACCCGTTTGGCTCC
18sRNA	5′-CCTGCGGCTTAATTTGACTCA	5′-AACTAAGAACGGCCATGCAC
Il6	5′-CCTCTCTGCAAGAGACTTCCATCCA	5′-AGCCTCCGACTTGTGAAGTGGT
Socs3	5′-ATGGTCACCCACAGCAAGTTT	5′-TCCAGTAGAATCCGCTCTCCT